Available online at www.sciencedirect.com
ScienceDirect
Journal of Power Sources 178 (2008) 795–800
JOURNAL OF POWER SOURCES
www.elsevier.com/locate/jpowsour

Short communication

# Fabrication and properties of a carbon/polypyrrole three-dimensional microbattery

Hong-Seok Min [a], Benjamin Y. Park [b], Lili Taherabadi [b], Chunlei Wang [c], Yuting Yeh [a], Rabih Zaouk [b], Marc J. Madou [b], Bruce Dunn [a,*]

[a] *Department of Materials Science and Engineering, University of California, Los Angeles (UCLA), Los Angeles, CA 90095, USA*
[b] *Department of Mechanical and Aerospace Engineering, University of California, Irvine (UCI), Irvine, CA 92697, USA*
[c] *Department of Mechanical and Materials Engineering, Florida International University, Miami, FL 33174, USA*

Received 26 July 2007; received in revised form 1 October 2007; accepted 2 October 2007
Available online 7 October 2007

**Abstract**

The carbon-microelectromechanical systems (C-MEMS) microfabrication process offers a promising method for fabricating three-dimensional (3D) battery architectures. In the current study, this approach was extended to the fabrication of positive electrode arrays and their assembly in a 3D lithium-ion microbattery. The positive electrode array was fabricated by electrochemical deposition of dodecylbenzenesulfonate-doped polypyrrole (PPYDBS) on an array of carbon rods. Electrochemical measurements show that the electrodeposited PPYDBS electrode array reversibly intercalates lithium with better gravimetric capacity than that of 2D electrodeposited films. The prototype carbon/PPYDBS 3D battery was based on an interdigitated electrode array configuration. It functioned as a secondary battery but the performance was limited because of electrical shorting. These initial results with the 3D interdigitated battery help to identify the needs associated with different electrode fabrication approaches and specific 3D designs.


*Keywords:* Three-dimensional battery; Microbattery; Carbon-microelectromechanical systems (C-MEMS); Polypyrrole

## 1. Introduction

Three-dimensional (3D) microbatteries have been proposed as a new direction for miniaturizing portable power sources [1]. The 3D configuration makes use of the out-of-plane dimension in contrast to traditional thin-film battery electrodes, which use only the in-plane surface. The use of the "vertical" dimension enables the battery to have a small areal footprint, which can be an important consideration for portable power applications. Another benefit of 3D architectures is the prospect of achieving high power density from maintaining a short ion diffusion length between anode and cathode and from high electrode surface area [1,2].

The fabrication and operation of both 3D battery structures and 3D battery electrodes have been reported recently for different battery systems. The use of 3D electrode arrays was reported recently for a nickel–zinc microbattery [3], a zinc–air microbattery [4] and carbon post electrodes for lithium-ion batteries [5–7]. In the latter studies, the individual posts were at least 10 μm thick. Another approach is that reported by Peled and coworkers where thin films were deposited in a 3D arrangement using a microchannel plate as the substrate [8,9].

One of the most promising methods for fabricating 3D architectures is to use carbon-microelectromechanical systems (C-MEMS). The C-MEMS approach offers an interesting material and microfabrication solution to the battery miniaturization problem [7,10–13]. In the C-MEMS process, photoresist is patterned by photolithography and subsequently pyrolyzed at high temperatures in an oxygen-free environment. By changing the lithography conditions, the soft and hard baking times and temperatures, and the pyrolysis treatment, C-MEMS lead to a variety of interesting new MEMS structures with a wide variety of shapes, electrical resistivity and mechanical properties. C-MEMS have already demonstrated the ability to fabricate high aspect ratio carbon electrode arrays for the reversible charge and discharge of lithium [7]. The ability to pattern carbon elec-

* Corresponding author. Tel.: +1 310 825 1519; fax: +1 310 206 7353.
*E-mail address:* bdunn@ucla.edu (B. Dunn).

0378-7753/$ – see front matter © 2007 Elsevier B.V. All rights reserved.
doi:10.1016/j.jpowsour.2007.10.003

trodes by photolithography is important for 3D battery designs as it enables fine control of electrode spacing and geometry in addition to the 3D electrode array configuration.

The present research addresses the important question of whether the C-MEMS fabrication process can move beyond the carbon anode (negative electrode) and be used to produce cathode (positive electrode) structures for 3D lithium-ion batteries. Our approach involved electrochemically depositing a second electrode material onto carbon posts and using this process in assembling an interdigitated 3D battery. To form the active material for the cathode, a dodecylbenzenesulfonate-doped polypyrrole (PPYDBS) was selected because it has a low specific weight, good chemical stability, adequate specific capacity, and, most importantly, can be electrochemically polymerized on one set of 3D carbon post arrays [14,15]. In this paper, we compare the electrochemical properties of 3D PPYDBS electrode arrays to those of the corresponding 2D films and demonstrate the functioning of an interdigitated 3D battery.

## 2. Experimental

### 2.1. 3D architecture fabrication

We have used the C-MEMS process to fabricate 3D Li-ion batteries consisting of arrays of carbon posts interdigitated with arrays of PPYDBS posts. Fig. 1 shows the fabrication procedure for the complete carbon/polymer battery. This fabrication process involves three steps: patterning the photoresist using photolithography; pyrolyzing the patterned photoresist to form carbon electrode arrays and carbon current collectors; and electrochemically polymerizing the PPYDBS on one set of 3D carbon arrays.

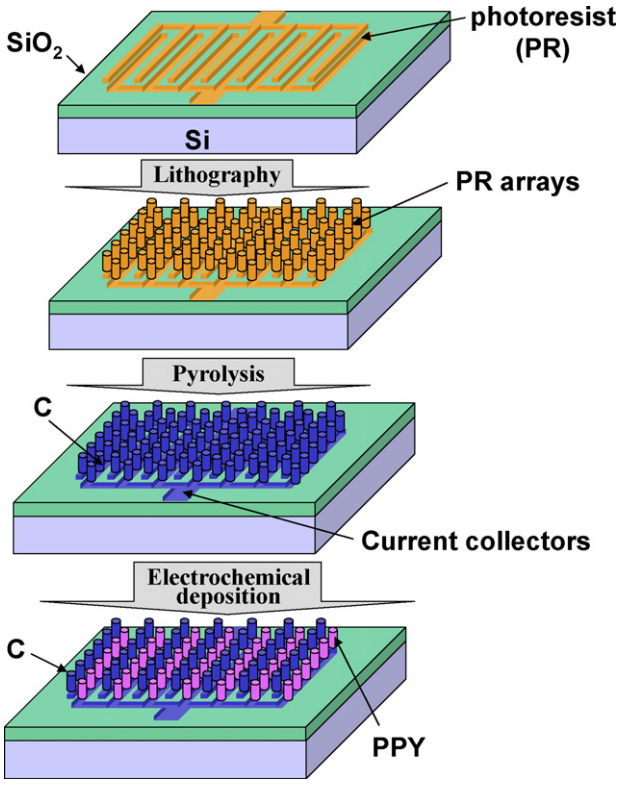


Fig. 1. Procedure for fabricating the carbon/polypyrrole three-dimensional battery. The area over which the rod array covers the silicon substrate represents the footprint area of the 3D electrode.

The electrode arrays and current collectors were fabricated by patterning a two-level SU-8 structure [13]. This photoresist was spin-coated onto a substrate of 500 nm of $SiO_2$ grown on Si. For producing the two-level structure, two kinds of mask designs were used to generate current collectors and posts: $120 \times 120$ arrays of fingers with 20 μm width and center to center distance of 120 μm, and $120 \times 120$ arrays of circles with 20 μm diameter and center to center distance of 85 μm, respectively. The photolithography process used for SU-8 photoresist patterning included spin coating, soft bake, near UV exposure, development, and post-bake [7].

After patterning the SU-8, the C-MEMS architectures were obtained using a two-step pyrolysis process in an open ended quartz-tube furnace. First, the samples were heated in $N_2$ atmosphere at 300 °C for about 40 min. The temperature was then increased at a rate of ∼10 °C $min^{-1}$ to 900 °C in flowing $N_2$ (flow rate of ∼2000 standard $cm^3$ $min^{-1}$ (sccm)). The atmosphere was then changed to forming gas [$H_2$ (5%)/$N_2$] also flowing at the 2000 sccm rate. The sample was kept at 900 °C for 1 h, then the heater was turned off and the samples were cooled in $N_2$ atmosphere until they reached room temperature when they were removed from the furnace.

All the PPYDBS films and arrays used in this study were synthesized by electrochemical polymerization of pyrrole in sodium dodecylbenzenesulfonate (NaDBS) aqueous solution [14]. Both the pyrrole (Aldrich, 98%) and the NaDBS salt (Aldrich) were used as received without further purification. The films were prepared by anodic oxidation of 0.1 M pyrrole monomer in the presence of 0.1 M aqueous sodium dodeclybenzenesulfonate. The 0.1 M NaDBS solution was made with de-ionized water as solvent and then was degassed by pumping nitrogen gas into the solution. To reduce the possibility of pyrrole degradation, the pyrrole polymerization solutions were prepared just prior to use by adding pyrrole to the premixed NaDBS solution, and then quickly mixing by gentle shaking. Electrochemical deposition was performed in a single compartment glass cell using a PC4/750 potentiostat (Gamry Instruments). Deposition was carried out in the galvanostatic mode using a constant current density of 0.1 mA $cm^{-2}$. A gold-coated silicon plate with a large surface area was used as a counter electrode for the polymerization and a Ag/AgCl electrode (Fischer Scientific) was used as the reference electrode. A uniform film of PPYDBS, about 10 μm thick, was obtained on the substrate after 1 h polymerization. After electrochemical deposition of the polymer, the structure was rinsed and dried with nitrogen. A Hitachi S-4700-2 field-emission SEM (FESEM) was used to provide images of the C-MEMS structures.

### 2.2. Electrochemical characterization

Two different types of electrodes were studied. One was an unpatterned PPYDBS film, 10 μm thick, which was electrochemically deposited, as discussed above, on a carbon-coated

$SiO_2$/Si wafer. This PPYDBS film was designed to serve as a reference sample to determine whether electrochemically polymerized PPYDBS exhibited reversible intercalation/de-intercalation of lithium. The second sample was a 3D electrode array obtained from C-MEMS microfabrication and PPYDBS electropolymerization. The 3D electrode consisted of a $120 \times 120$ square array of posts with a post height of $\sim$65 μm. The footprint area of the 3D electrode was 1 $cm^2$. All the test cells were assembled and tested in an argon filled glove box in which both the oxygen and moisture levels were less than 1 ppm. Cyclic voltammetry (CV) and galvanostatic charge/discharge experiments were carried out on both types of cells using an electrolyte of 1 M $LiClO_4$ in a 1:1 volume mixture of ethylene carbonate (EC) and dimethyl carbonate (DMC).

Electrochemical measurements were carried out on 2D PPYDBS films, 3D electrode arrays of PPYDBS, 3D electrode arrays of carbon and the full C/PPYDBS 3D battery. The measurements made on PPYDBS films used a two-electrode Teflon cell that employed an O-ring seal to define the working electrode to 7 $cm^2$. The PPYDBS film served as the working electrode and lithium ribbon (99.9% pure, Aldrich) was used as the counter electrode. We tested the 3D carbon electrode arrays and the 3D PPYDBS electrode arrays separately using the C/PPYDBS interdigitated structure. The 3D electrode arrays of both PPYDBS and carbon were characterized in three-electrode experiments in which lithium foils served as reference and counter electrodes. The 3D C/PPYDBS full battery was tested in a two-electrode arrangement in which the PPYDBS array served as the working electrode and the carbon array was the counter electrode. Prior to battery operation, the carbon electrode arrays were intercalated with $Li^+$ from the previous half-cell experiments.

For the CV measurements, the potential was scanned from 3.7 to 2.1 V vs. $Li/Li^+$ for PPYDBS and from 3.2 to 0.01 V vs. $Li/Li^+$ for carbon. The scan rate was fixed at 1 mV/s for PPYDBS and 0.5 mV $s^{-1}$ for carbon. For galvanostatic charge–discharge cycling measurements, the PPYDBS electrode operated between 2.2 and 3.8 V vs. $Li/Li^+$, while the carbon electrode was operated between 0.01 and 3 V vs. $Li/Li^+$. The charge and discharge current densities for testing the C/PPYDBS 3D battery were 90 μA $cm^{-2}$ (2.1 C) and 20 μA $cm^{-2}$ (0.46 C), respectively. In all experiments involving 3D electrodes, the reference area is that of the footprint area of the electrode post array, 1 $cm^2$. The electrochemical measurements were carried out using either an EG&G Princeton Applied Research Model 273 potentiostat or an Arbin BT4 potentiostat/galvanostat.

## 3. Results and discussion

### 3.1. 3D battery structures of carbon/PPYDBS

A 3D battery structure composed of interdigitated arrays of carbon and PPYDBS rods was fabricated successfully (Fig. 2). The arrays are uniform with straight walls and good edge

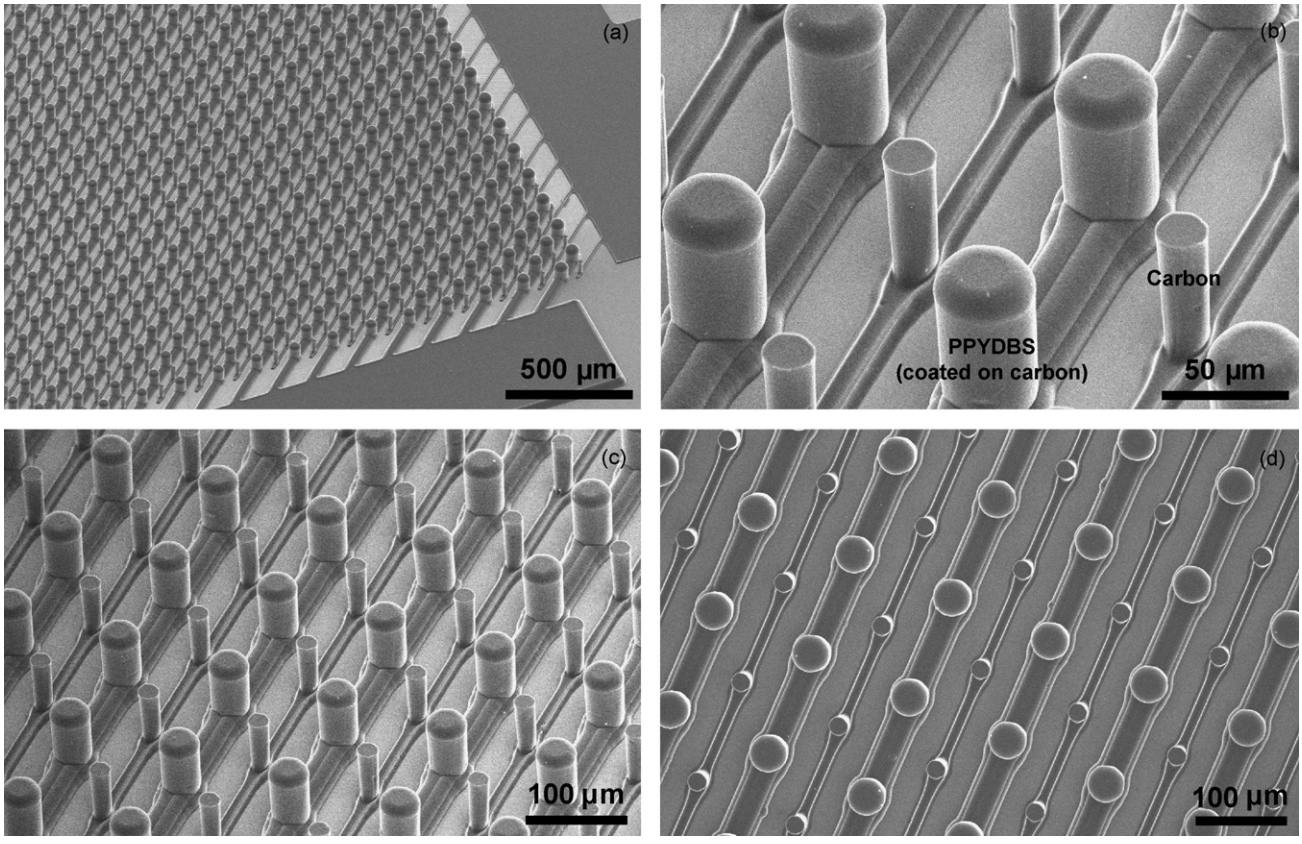


Fig. 2. SEM images of C/PPYDBS post arrays. The thicker electrode is the PPYDBS and the thinner electrode is carbon; (a), (b) and (c) tilt views and (d) top view of arrays.

Table 1
Values for various parameters of the 3D C/PPYDBS microbattery

| Parameter | 3D C/PPYDBS arrays | |
|---|---|---|
| | Carbon electrodes | PPYDBS electrodes |
| Footprint area | 1 $cm^2$ | 1 $cm^2$ |
| Finger area | 0.17 $cm^2$ | 0.35 $cm^2$ |
| Rod height | 61.8 μm | 64.9 μm |
| Rod diameter | 19.1 μm | 39.3 μm |
| Volume | $2.12 \times 10^{-4}$ $cm^3$ | $5.47 \times 10^{-4}$ $cm^3$ |
| Mass | 0.423 mg | 0.82 mg |

profiles. Values for the average height and diameter for the carbon and PPYDBS rods are listed in Table 1. The aspect ratio (height/width) for the carbon and PPYDBS electrodes is 3.2:1 and 1.7:1, respectively. Because the PPYDBS was electrodeposited on carbon posts, in determining the volume of PPYDBS, it is necessary to subtract the volume of the carbon posts from the total volume. From the volume of carbon and PPYDBS, we calculated the weight of active materials based on the theoretical density of carbon and PPY, which are 2 and 1.5 g $cm^{-3}$ [16,17], respectively. Thus, we are able to use the gravimetric capacity to compare the 2D and 3D PPYDBS electrodes and determine whether electrode geometry has any effect on electrochemical properties.

We estimated the capacity for the 3D C/PPYDBS microbattery based on the specific capacity values we measured for the individual 3D electrode arrays as described below and listed in Table 2. Because one of the attractive features of 3D architectures is that of obtaining a small footprint area for the battery, we area-normalize the specific capacity (termed the areal capacity) to the footprint area rather than use traditional gravimetric or volumetric normalization [2]. The footprint area of the 3D electrode arrays was 1 $cm^2$ as defined by the area that the electrode covered on the silicon substrate (see Fig. 1). All of the 3D electrode structures, including both half-cells and full cells, had the same footprint area.

### 3.2. Characterization of PPYDBS films

Fig. 3 shows the results of the charge/discharge tests at different current densities for the 2D PPYDBS film. Based on the specific capacity reported for PPYDBS (53 mAh $g^{-1}$) [14], the charge/discharge experiments were carried out at rates of 0.09 C (7.1 μA $cm^{-2}$), 0.36 C (28.6 μA $cm^{-2}$), and 0.9 C (71.4 μA $cm^{-2}$). The highest capacity is observed at 0.09 C, however, the capacities exhibit only about a 10% decrease

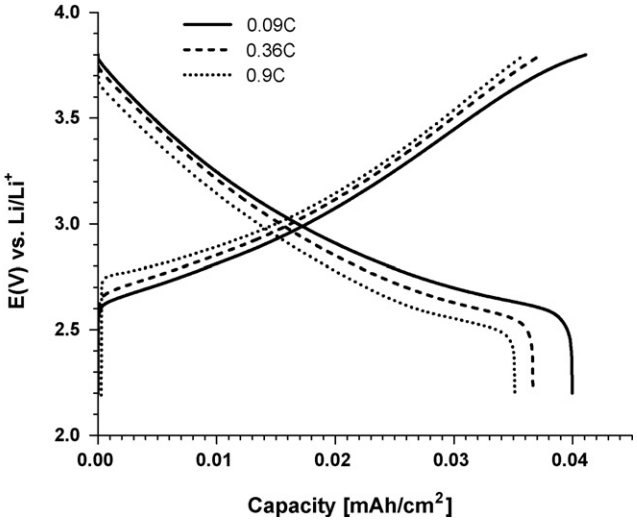


Fig. 3. Charge/discharge characteristics for the 2D PPYDBS film. The electrolyte is 1 M $LiClO_4$ in 1:1 EC-DMC. The current densities are ±7.1 μA $cm^{-2}$ (0.09 C), ±28.6 μA $cm^{-2}$ (0.36 C), and ±71.4 μA $cm^{-2}$ (0.9 C).

for a 10-fold increase in current density. When we normalize the lithium capacity to the area of the electrode (7 $cm^2$), we find that the corresponding areal energy densities are 40, 36.7, and 35.1 μAh $cm^{-2}$ for 0.09, 0.36, and 0.9 C, respectively. We used these results to estimate the gravimetric capacity for the PPYDBS film by knowing the film thickness (10 μm) and polypyrrole density (1.5 g $cm^{-3}$) [16,17]. For a fully dense film, this corresponds to 26.7 mAh $g^{-1}$ (at 0.09 C), which is 50% of the value reported for PPYDBS (53 mAh $g^{-1}$) [14]. Despite the limited specific capacity of the PPYDBS film, the more important feature here is that the PPYDBS can be electrochemically polymerized on a carbon substrate and used as the positive electrode in a rechargeable lithium-ion battery. According to Scrosati and co-workers, the reactions involved in the PPYDBS film can be represented by [14]:

$$(\mathrm{PPy} + \mathrm{DBS}^-) + n\mathrm{Li}^+ + n\mathrm{e}^- \underset{\text{charge}}{\overset{\text{discharge}}{\rightleftarrows}} (\mathrm{PPyDBS}^-\mathrm{Li}^+) \quad (1)$$

$$n\mathrm{Li}^0 \underset{\text{charge}}{\overset{\text{discharge}}{\rightleftarrows}} n\mathrm{Li}^+ + n\mathrm{e}^- \quad (2)$$

Reactions (1) and (2) are in the cathode (positive electrode) and anode (negative electrode), respectively. During discharge, the PPYDBS film is reduced upon insertion of $Li^+$ ions in order to maintain electroneutrality. Simultaneously, the lithium negative electrode is oxidized with dissolution

Table 2
Calculated and experimental capacity values for PPYDBS films, 3D electrode arrays and the 3D C/PPYDBS microbattery

| Materials (test condition) | Calculated values | | Experimental results | |
|---|---|---|---|---|
| | Specific capacity | Areal capacity | Gravimetric capacity | Areal capacity |
| 2D PPYDBS (half-cell) | 53 mAh $g^{-1}$ [14] | 79.5 μAh $cm^{-2}$ | 23.4 mAh $g^{-1}$ | 35.1 μAh $cm^{-2}$ |
| 3D PPYDBS (half-cell) | 53 mAh $g^{-1}$ [14] | 43.5 μAh $cm^{-2}$ | 37.9 mAh $g^{-1}$ | 31 μAh $cm^{-2}$ |
| 3D carbon (half-cell) | 220 mAh $g^{-1}$ [13] | 93.1 μAh $cm^{-2}$ | 136 mAh $g^{-1}$ | 57.6 μAh $cm^{-2}$ |
| 3D C/PPYDBS (full cell) | – | 43.5 μAh $cm^{-2}$ | – | 10.6 μAh $cm^{-2}$ |

of $Li^+$ ions in the electrolyte. During charge, the opposite occurs.

### 3.3. Characterization of 3D electrode arrays

The 3D PPYDBS electrode exhibits similar electrochemical behavior to that of the PPYDBS film as shown in Fig. 4. There is no question that the 3D PPYDBS array is electrochemically reversible for lithium. In comparing the gravimetric capacities for the 2D and 3D PPYDBS at approximately the same C-rate (0.9 and 1.15 C, respectively) we find that the 3D PPYDBS electrode array exhibits a much higher gravimetric capacity (37.9 mAh $g^{-1}$ at 1.15 C) than 2D PPYDBS films (23.4 mAh $g^{-1}$ at 0.9 C). One contribution to the larger gravimetric capacity arises from the larger active surface area of 3D electrode array. Another consideration is that with the 3D array configuration, the electrolyte penetrates the entire electrode as compared to the planar front that the electrolyte makes with the 2D PPYDBS electrode.

The voltammetric sweeps used to characterize the intercalation/de-intercalation of lithium in the 3D carbon electrode array (Fig. 5) exhibit certain features similar to those of the carbon electrode arrays reported by Wang et al. [7]. The response below 2.0 V is analogous to that reported by Ma et al. with most of the $Li^+$ intercalation occurring at potentials less than 0.5 V and a broad de-intercalation peak centered at 0.3 V [18]. However, it is important to note that at higher potentials, PPYDBS redox reactions are observed in the scan range between 2.1 and 3.2 V. These reactions suggest that electrical leakage occurs between the carbon and PPYDBS arrays, an effect which limits the operation of the battery (*vide infra*). This response is not apparent in the galvanostatic measurements of the 3D carbon arrays (Fig. 6) made at 50 μA $cm^{-2}$ where the irreversible capacity on the first discharge is followed by good cycling behavior. The area normalized discharge capacity for the 3D carbon electrode array is 57.6 μAh $cm^{-2}$. This value is larger than that of the 3D PPYDBS electrode (31 μAh $cm^{-2}$), suggesting that the areal energy density of a 3D C/PPYDBS microbattery is likely to be determined by the capacity of the positive electrode.

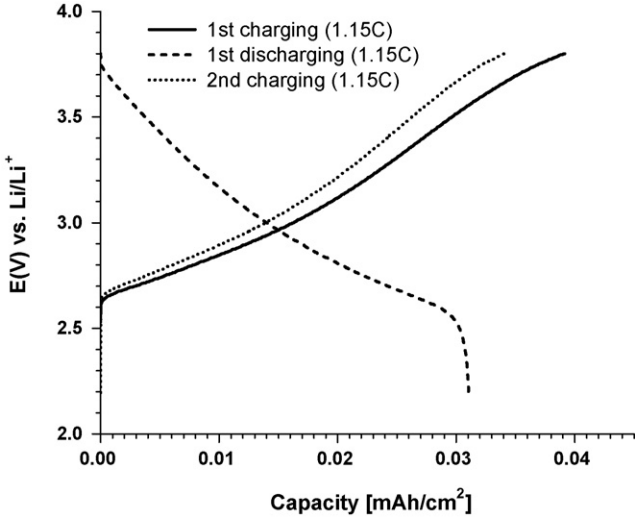


Fig. 4. Charge/discharge characteristics for the 3D PPYDBS array. The electrolyte is 1 M $LiClO_4$ in 1:1 EC-DMC. The current density is ±50 μA $cm^{-2}$ (1.15 C).

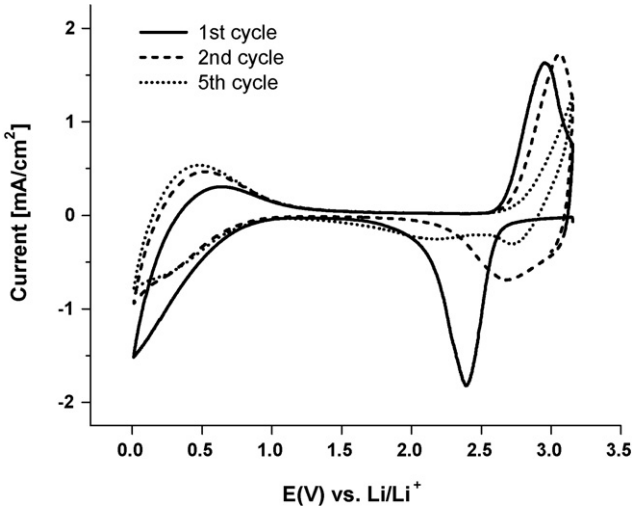


Fig. 5. Cyclic voltammograms for the 3D carbon array. The electrolyte is 1 M $LiClO_4$ in 1:1 EC-DMC and the sweep rate is 0.5 mV $s^{-1}$.

### 3.4. Characterization of the carbon/PPYDBS 3D microbattery

The prototype of the 3D C/PPYDBS microbattery was cycled galvanostatically at a discharge rate of 20 μA $cm^{-2}$ (0.46 C) for a total of 12 cycles. The first three cycles are shown in Fig. 7. The charge/discharge behavior demonstrates that the 3D C/PPYDBS microbattery functions as a secondary battery which exhibits reversible intercalation/de-intercalation of lithium. The areal capacity of 10.6 μAh $cm^{-2}$ is only about one-third of the areal capacity expected based on the individual electrode arrays (Table 2). A more serious problem, however, is evidence of electrical shorting as there is considerably more charge than discharge observed with this battery (Fig. 7). The origin of the short

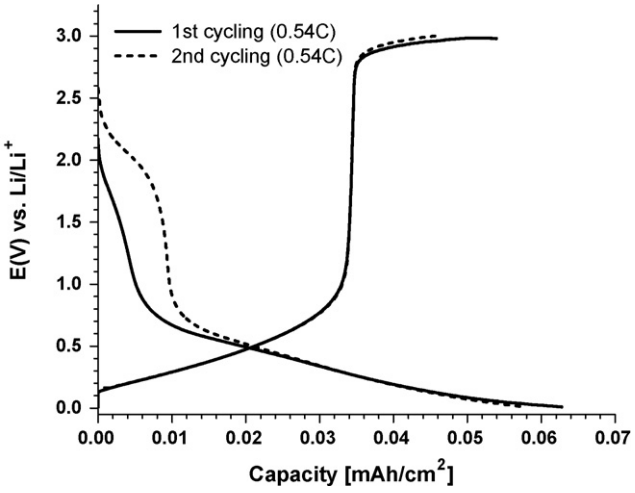


Fig. 6. Charge/discharge characteristic for the 3D carbon array. The electrolyte is 1 M $LiClO_4$ in 1:1 EC-DMC. The current density is ±50 μA $cm^{-2}$ (0.54 C).

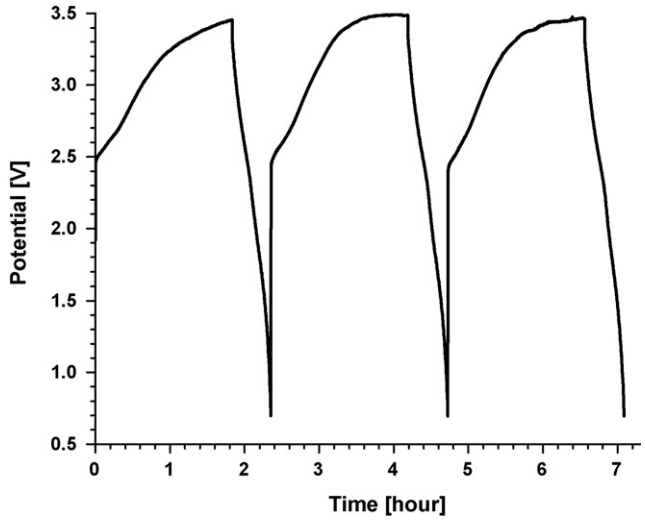


Fig. 7. Charge/discharge characteristic for the 3D C/PPYDBS interdigitated microbattery. The electrolyte is 1 M $LiClO_4$ in 1:1 EC-DMC. The discharge current is 20 $\mu A\,cm^{-2}$ (0.46 C) and the charge current is 90 $\mu A\,cm^{-2}$ (2.1 C).

is not exactly clear, although as shown in Fig. 5, there is a current path established between the two interdigitated electrodes. One possibility is that PPYDBS may be deposited beyond the defined area and extend laterally from the cathode posts to the anode posts forming a low resistance path, leading to self-discharge. It should be noted that this specific 3D battery architecture does not contain a separator and suggests that the combination of the interdigitated configuration and C-MEMS fabrication may require a separator if this approach is to prove successful.

The internal short may have masked another potential problem, that of a high internal resistance which arises from the fact that the resistivity of the carbon current collector is nearly one order of magnitude higher than that of copper. As shown in Figs. 1 and 2, the carbon and PPYDBS posts are attached to carbon "fingers" that serve as current collectors. The fingers are some 19 μm wide and 5 μm thick, thus, its linear ohmic resistance drop is about 13.4 $k\Omega\,cm^{-1}$. At the charge/discharge rates investigated here, this high internal resistance would lead to an overpotential and decrease the amount of $Li^+$ intercalation/de-intercalation accordingly. The extent to which high internal resistance affected 3D battery performance in our experiments could not be established.

## 4. Conclusion

The C-MEMS microfabrication process offers a lithographically patterned approach for the fabrication of 3D carbon electrode arrays. In this study, we have shown that by using electrochemical deposition the C-MEMS processing method can be extended to fabricating arrays of a positive electrode material for lithium-ion batteries. The electrochemical properties of the positive electrode material, PPYDBS, were compared in both 2D and 3D configurations. The 3D PPYDBS array electrode exhibited reversible intercalation/de-intercalation with better gravimetric capacity than the electrodeposited 2D films. Moreover, the use of electrodeposition enabled us to construct a 3D microbattery of C/PPYDBS based on an interdigitated electrode design. The battery was able to function, however its operation was limited because of an electrical short. Despite this response, this is an important result for the emerging 3D battery technology as it identifies the shortcomings and needs associated with different electrode fabrication approaches and specific 3D designs.

## Acknowledgment

We greatly appreciate the support of our research by the Office of Naval Research.

## References

[1] R.W. Hart, H. White, B. Dunn, D. Rolison, Electrochem. Commun. 5 (2003) 120–123.
[2] J.W. Long, B. Dunn, D. Rolison, H.S. White, Chem. Rev. 104 (2004) 4463–4492.
[3] F. Chamran, Y. Yeh, H.-S. Min, B. Dunn, C.-J. Kim, J. Microelectromech. Syst. 16 (2007) 844–852.
[4] F. Chamran, H.-S. Min, B. Dunn, C.-J. Kim, Proc. 20th IEEE Int. Conf. Micro Electro Mechanical Systems (MEMS'07), Kobe, Japan, January 21–25, 2007, pp. 871–874.
[5] F. Chamran, U.-C. Yi, C.-J. Kim, Proc. Solid-State Sensors Actuators and Microsystem Workshop (Hilton Head'06), Hilton Head Island, SC, USA, June 5–8, 2006, pp. 185–188.
[6] F. Chamran, Y. Yeh, B. Dunn, C.-J. Kim, Proc. ASME Int. Mech. Eng. Congress and Exposition (IMECE 2004), Anaheim, CA, USA, November 13–19, 2004 (IMECE 2004-61925).
[7] C. Wang, L. Taherabadi, G. Jia, M. Madou, Y. Yeh, B. Dunn, Electrochem. Solid State Lett. 7 (2004) A435–A438.
[8] D. Golodnitsky, M. Nathan, V. Yufit, E. Strauss, K. Freedman, L. Burstein, A. Gladkich, E. Peled, Solid State Ionics 177 (2006) 2811–2819.
[9] M. Nathan, D. Golodnitsky, V. Yufit, E. Strauss, T. Ripenbein, I. Shechtman, S. Menkin, E. Peled, J. Microelectromech. Syst. 14 (2005) 879–885.
[10] S. Ranganathan, R. McCreery, S.M. Majji, M. Madou, J. Electrochem. Soc. 147 (2000) 277–282.
[11] K. Kinoshita, X. Song, J. Kim, M. Inaba, J. Power Sources 81–82 (1999) 170–175.
[12] J. Kim, X. Song, K. Kinoshita, M. Madou, R. White, J. Electrochem. Soc. 145 (1998) 2314–2319.
[13] C. Wang, G. Jia, L.H. Taherabadi, M.J. Madou, J. Microelectromech. Syst. 14 (2005) 348–358.
[14] R.C.D. Peres, M.A. De Paoli, S. Panero, B. Scrosati, J. Power Sources 40 (1992) 299–305.
[15] S. Panero, E. Spila, B. Scrosati, J. Electrochem. Soc. 143 (1996) L29–L30.
[16] A.F. Diaz, J.I. Castillo, J.A. Logan, W.-Y. Lee, J. Electroanal. Chem. 129 (1981) 115–132.
[17] J. Tietje-Giraulta, C. Ponce de Leónb, F.C. Walsh, Surf. Coat. Technol. 201 (2007) 6025–6034.
[18] S. Ma, J. Li, X. Jing, F. Wang, Solid State Ionics 86–88 (1996) 911–917.